Chalcogenide Letters Vol. 22, No. 3, March 2025, p. 239 - 253

Enhancement of performance $Cd_xPb_{1-x}S$ / porous silicon heterojunction photodetector by chemical spray pyrolysis method

S. I. Aziz, G. G. Ali *
Physics Department, College of Education for Pure Science, Mosul University, Iraq

This work investigates the photodetector characteristics of lead and cadmium sulfide thin films deposited on porous silicon heterojunction at composites (x=0,0.25,0.5,0.75,1). The characteristics of all deposited samples were estimated by X-ray diffraction (XRD), high-resolution scanning electron microscope (FESEM), Energy-dispersive X-ray (EDX), I-V measurements, and photodetector properties. PbS and CdS thin films have been successful, and photodetector properties on the porous silicon surface have performed well using the chemical spray method. An X-ray confirmed that the prepared samples have a crystalline phase structure. Besides, the results indicate that the PbS and CdS thin films have cubic and hexagonal structures respectively. In detail, the crystalline size decreases with increasing concentration. FESEM images show that the porous silicon has a sponge-like structure and is uniformly distributed at the surface. Furthermore, I-V curves of the prepared thin films have rectifying behavior. The performance of $Cd_xPb_{1-x}S$/ Porous silicon as a photodetector shows that the maximum values of quantum efficiency were found to be 10%, 14%, 16%, 23%, and 44% at x=0,0.25,0.5, 0.75and 1 respectively. The variation of photocurrent with time (time rise and time fall) has good electrical stability and fast response under light cycling. The photodetector performance of $Cd_xPb_{1-x}S$/ Porous silicon heterojunction is in a positive linear relationship with the used concentration.

(Received December 21, 2024; Accepted March 12, 2025)

Keywords: CdS, PbS , Porous silicon, I-V measurements, Photodetector

1. Introduction

The Lead and cadmium sulfate exhibit promise in numerous of devices that have received great attention in many applications such as gas sensors [1], photoconductors, solar cells, filters, light emitting diode and optical switches [2]. It can be seen, the lead sulphide (PbS) has cubic crystal structure and a narrow direct band gap of 0.41 to 4 eV with high absorption coefficient of 10^5 cm^{-1} at room temperature. Furthermore, the PbS compound belongs to the IV-VI group of semiconductors [3]. Also, cadmium sulfate (CdS) is a expand bandgap of 2.43 eV and is one of the main optimum materials for window layer in photovoltage applications due to its high refractive index and efficient transport properties [4]. CdS have a hexagonal or cubic. Furthermore, the CdS thin film forms of a NaCl structure. Similarity, the PbS has cubic crystal structure according to crystalline system [5]. The mixture performance $Cd_xPb_{1-x}S$ thin film structure is important parameter due to unique physical and optical properties [6]. Compatible, the prepared films can be deposited under several methods such as chemical spray, sputtering, chemical bath (CBD), laser ablation, spin coating, chemical vapor deposition (CVD), physical vapor deposition (PECVD) and sol-gel [7]. Chemical spray method is one of the important techniques to deposit various materials as thin films in order to give high uniform thin film at the substrate [8]. Subsequently, the photoluminescence of porous silicon has been discovered in a previous decade by Canham (1990) [9]. The porous silicon has direct band gap semiconductor and has strong quantum confinement properties [10]. In recent years, there are numerous works published of porous silicon as photodetector material due to large surface area and low reflection index [11]. The photo-electrochemical etching technique is one of the important method to form uniform pores on silicon surface [12]. Besides, the combination between the mixture of CdS, PbS thin films and deposited

*Corresponding author: dr.ghazwan39@uomosul.edu.iq
https://doi.org/10.15251/CL.2025.223.239

on porous silicon substrate are necessary studies and used to many applications such as antireflection coating and transistors devices [13]. The objective work in this paper is to study the structure properties (XRD), Topography properties (FESEM), electrical properties(I-V) and photodetector devices.

2. Experimental method

2.1. Preparation of CdS and PbS nanocomposites

The cadmium sulfide (CdS) and the lead sulfide (PbS) thin films were prepared in a reaction solution containing cadmium chloride $CdCl_2$ (0.1 M), as a reference of ions Cd^{+2} and lead chloride $PbCl_2$ (0.1M) as a reference of ions Pb^{+2}. Sodium sulfide (Na_2S) as a reference of ions S^{-2} were Sigma Aldrich company. Cadmium solution and lead solution or one of them were tested by 80°C with magnetic stirring device for 2hr.In the beginning time, the color of CdS aqueous transform to the light yellow at 20min. After that, the color of the solution becomes darker and changed to dark yellow to orange within 2hr. Similarity, the color of PbS solution was light gray at 25min. Then, the color of the solution becomes darker and changed to dark gray to black within 2hr.The weight composites of cadmium and lead sulfide solutions were prepared at (x=0,0.25,0.5,0.75 and 1) .The first time the color of $Cd_{0.25}Pb_{0.75}$ S was light yellow at 18min and becomes to dark gray at 28min.the color of solution $Cd_{0.5}Pb_{0.5}S$ was light also yellow at 17min and becomes dark gray at 23min .Furthermore, the color of solution $Cd_{0.75}Pb_{0.25}$ S was light green at 12min and becomes to dark green at 24min. All solutions were mixed and heated at 90°. $Pb_{1-x}Cd_xS$ thin films were doped on glass substrates by the spray chemical technique at 250°C and an atmospheric pressure of 6.5 bar as the Figure1(a,b,c). The reaction was evaluation by the following equation [14]:

$$Na_2S(aq)+CdCl_2(aq) \longrightarrow CdS(s) + 2NaCl\ (aq) \quad (1)$$

$$Na_2S(aq)+PbCl_2(aq) \longrightarrow PbS(s) + 2NaCl\ (aq) \quad (2)$$

(a) (b) (c)

Fig. 1. (a) Solution of CdS and PbS, (b) Solution of composites $Cd_xPb_{1-x}S$ thin films (c) Chemical spray pyrolysis.

2.2. Set up and preparation of porous silicon substrate

Silicon wafers substrates of p-type (111) were used in (Germany company) with resistivity of (1–8 ohm. cm) using photo-electrochemical etching. Silicon wafer was cut off as small samples (2×2 cm) and cleaning with alcohol solution by an ultrasonic bath for 10 min and then rinsed with deionized water. The cell of porous silicon fabrication was made of Teflon plastic as cylinders shape. The set up consist of electric circuit containing Voltmeter, Ammeter and power supply. The

cathode electrode contains gold mash and the anode electrode as steel metal circle as Figure 2(b,c). All the samples immersed in mixed of hydrofluoric acid (16%HF) and ethanol (99%) solutions. The parameters conditions were used from current density (10mA/cm^2), the etching time (5,10,15min).

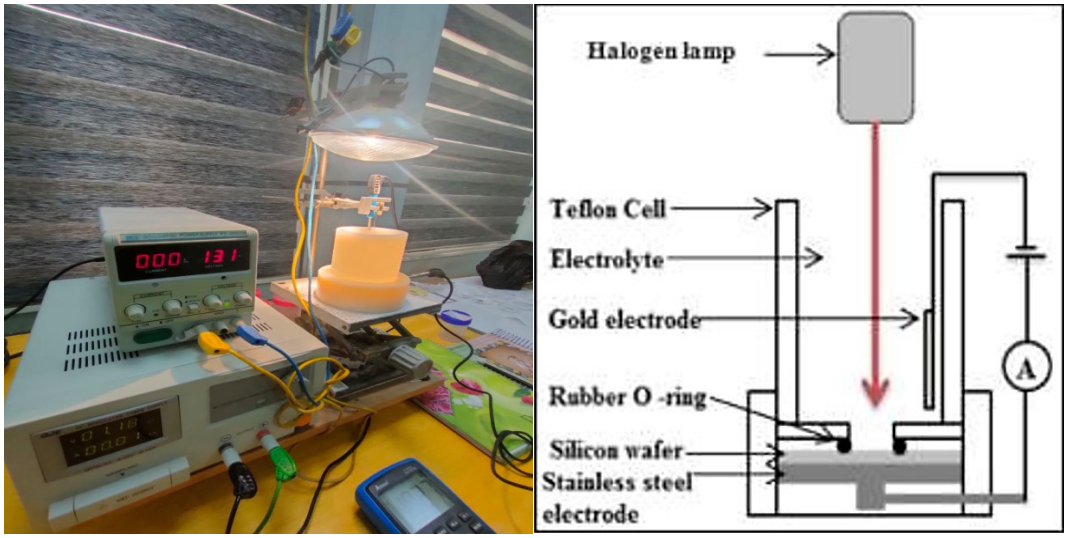

Fig. 2. (a) Photograph of the Photo electrochemical method, (c) Set up Photo electrochemical method.

3. Results and discussion

3.1. Structure properties

The XRD patterns of lead and cadmium sulphide thin films nanocomposites were studied on porous silicon substrates of various weight ratio at (x=0,0.25,0.5,0.75,1) as Figure 3. All the spectra of crystalline phase exhibit that the peaks of porous silicon have cubic crystal structure with a preferred crystalline orientation along the (111) [15]. The XRD analysis illustrated that the films of PbS and CdS exhibited a polycrystalline structure. It can be observed that the lead sulphide (PbS) thin film has cubic crystal structure related to (100), (111), (200), (222), (204) recorded at 2θ angles 26.72º,28.44º,39.73º,59.3º,84.44º respectively and corresponding to JCPDS Card No. (96-901-3403) [16]. Meanwhile, the weak diffraction signals were observed with increasing doping of Cd^{2+}. This refers to that the pattern of cadmium sulphide (CdS) has hexagonal phase structure orientation (002) belongs to 2θ =31.31º and corresponding to JCPDS Card No. (95-99-96-900-8840) [17]. It can be seen the angles (2θ) were shifted towards a small angle with increasing doping Cd^{2+} as Table1. The intensity of diffraction peaks increases with increasing doping of Cd^{2+}. The crystallite size of PbS and CdS thin films nanocomposites was evaluated through the Sherrer equation [18].

$$L = \frac{k\lambda}{B\cos\theta} \tag{3}$$

where L is the nanocrystal size, λ is the wavelength of XRD, β is the peak in radian of the full width at half maximum (FWHM), and θ is the angle of Bragg. It can be observed that the crystalline diameter decreases with doping Cd^{+2} of all spectra analysis. Additionally, the diffraction peaks become broadening with increasing doping of Cd^{2+} [19].

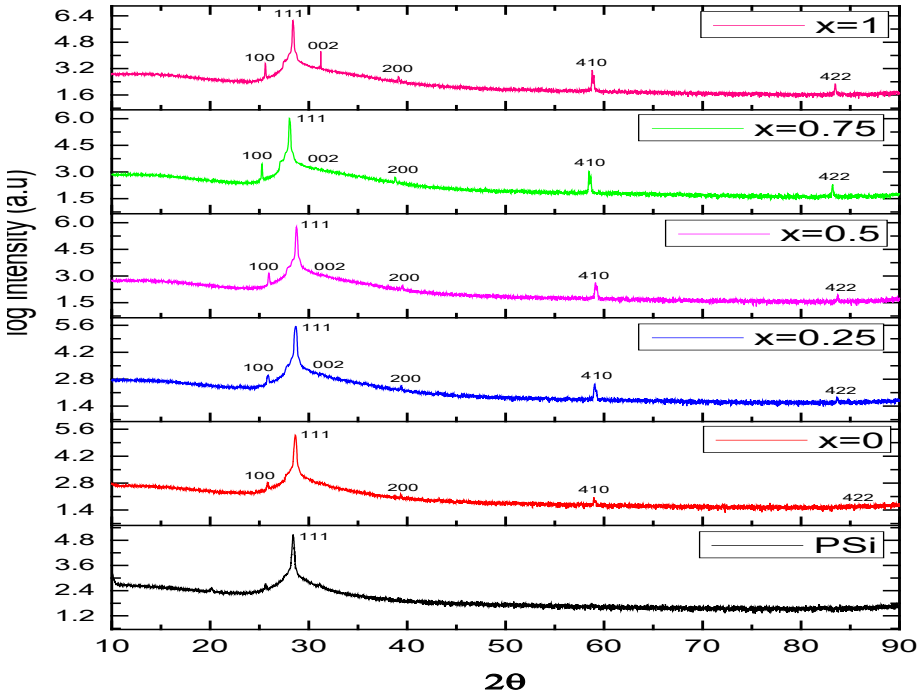

Fig. 3. XRD of $Cd_xPb_{1-x}S$/ Porous silicon thin films at different concentrations.

Table 1. Crystalline size, FWHM, inter-plane distance (d) of $Cd_xPb_{1-x}S$/ Porous silicon thin films.

Sample	2θ	*hkl*	*L*(nm)	FWHM (deg)	d (Aº)
Pure PSi	28.59	111	14.62	0.732	1.861
PbS/PSi	26.72	100	16.32	0.642	1.796
	28.44	111	14.34	0.751	1.978
	39.73	200	13.52	0.842	2.128
	59.3	222	14.26	0.781	2.015
	84.44	204	18.54	0.582	1.649
$Cd_{0.25}Pb_{0.75}S$/PSi	26.68	100	16.22	0.631	1.738
	28.39	111	14.31	0.764	2.032
	31.42	002	16.12	0.682	1.751
	39.62	200	13.46	0.821	2.242
	59.61	222	14.22	0.724	2.131
	84.37	204	18.47	0.572	1.771
$Cd_{0.5}Pb_{0.5}S$/PSi	26.61	100	16.17	0.582	1.643
	28.33	111	14.26	0.772	2.188
	31.37	002	15.97	0.671	1.781
	39.53	200	13.41	0.798	2.341
	59.56	222	14.16	0.713	2.186
	84.33	204	18.36	0.572	1.814
$Cd_{0.75}Pb_{0.25}S$/PSi	26.56	100	16.11	0.521	1.521
	28.22	111	14.21	0.833	2.219
	31.33	002	15.87	0.664	1.821
	39.46	200	13.38	0.742	2.462
	59.54	222	14.12	0.695	2.231
	84.27	204	18.22	0.567	1.834
CdS/PSi	26.51	100	15.89	0.511	1.431
	28.31	111	14.16	0.812	2.321
	31.31	002	15.71	0.639	1.851
	39.34	200	13.22	0.711	2.591
	59.43	222	13.97	0.715	2.312
	84.21	204	18.12	0.561	1.893

3.2. High-resolution Scanning electron microscope (FESEM)

The surface morphology (FESEM) of $Cd_xPb_{1-x}S$ thin films deposited on porous silicon substrates using chemical spray method with different composites ratio was investigated. The distribution of grain size of PbS thin film was observed as Figure4a. It can be seen that the particle size as dark color and spherical shape with uniform distribution [20] and the average diameter was 89nm. Besides, the average particle diameter of CdS thin film as light color was found to be (65nm) was observed as Figure 4b.

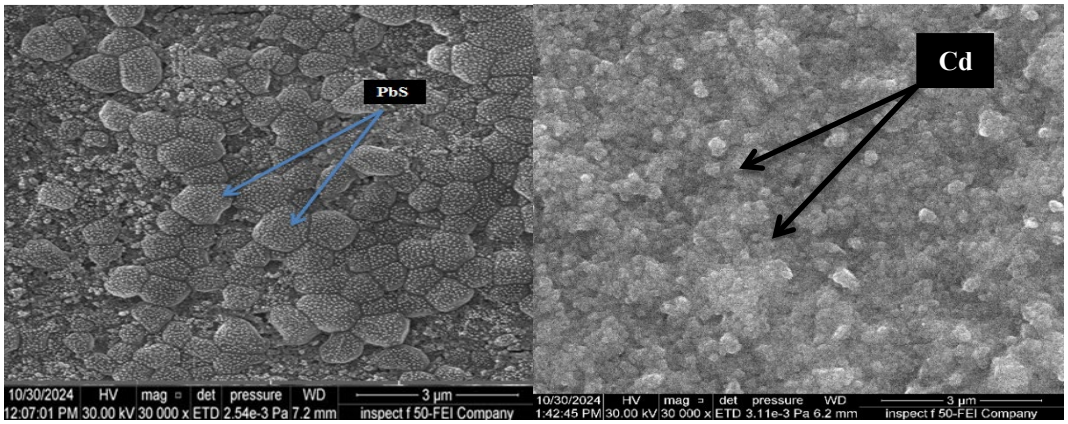

(a) *(b)*

Fig. 4. Images of SEM (a) PbS thin film, (b) CdS thin film.

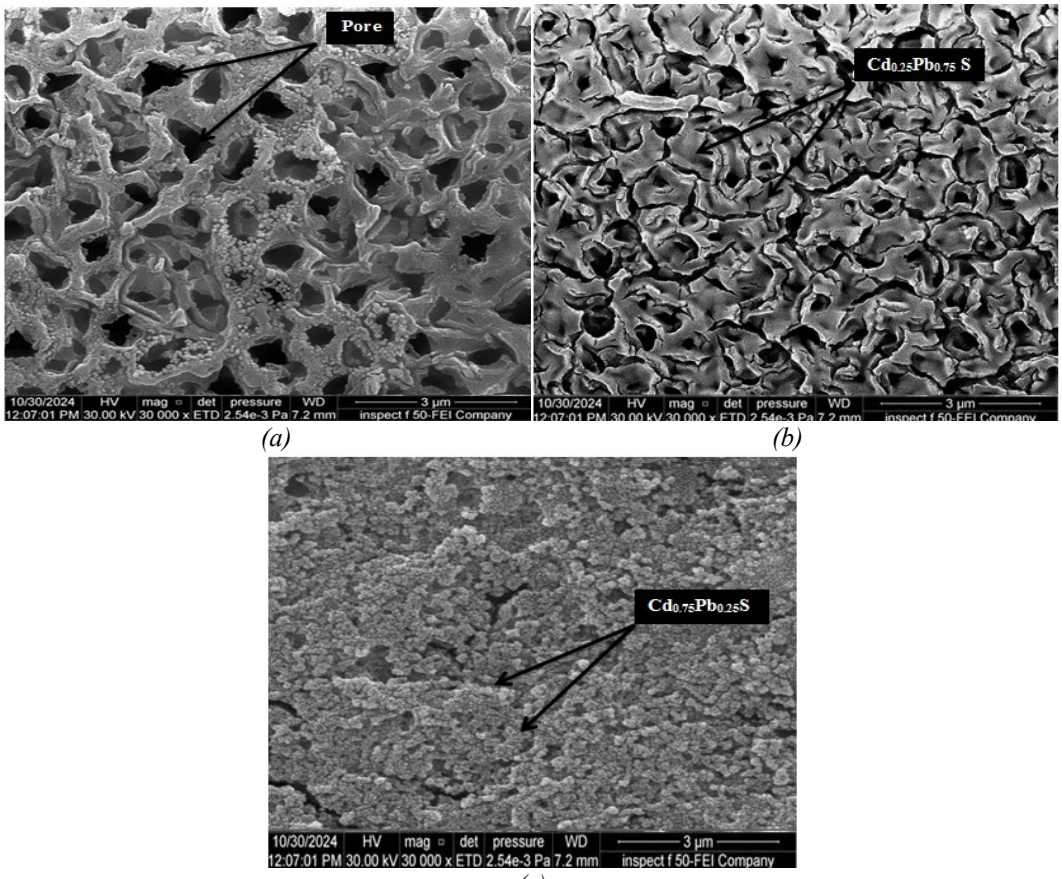

(a) *(b)*

(c)

Fig. 5. SEM of $Cd_xPb_{1-x}S$/porous silicon (a) PSi at etching 5min, (b) x=0.25 (c) x=0.75.

Furthermore, the surface of porous silicon has sponge-like structure [21]and the pore size of porous silicon domains as spherical shape with uniform randomly at etching time 5min as Figure 5a. On the other hand, Figure 5(b,c) indicates that the cadmium and lead sulphide nanocomposites occupy partially only some of the pores of the porous silicon surface[22]. Furthermore, the nucleation and growth processes are prolonged, ensuring a well-defined matrix with strong coagulation of particle size together [23]. The average pore diameter was found to be 0.62µm and 0.71µm at composites x=0.25,0.75 respectively. Similarity, the pore size increases with increase etching time at (15min) and the pore diameter becomes larger as well as the wall around pore reduce as Figure 6a. The formation of particle size is homogenous distribution with gradually increasing Cd^{2+}. The growth mechanisms of the particle size as cluster mechanism as Figure 6(b,c). The average pore diameter was found to be 1.09µm and 1.24µm at composites x=0.25,0.75 respectively. The cross section of the composites $Cd_xPb_{1-x}S$ thin films formed on porous silicon at x= 0.75 at various magnification was displayed as Figure 7(a,b,c,d) .It can be noted , the grain size of the thin film was agglomerated on the porous silicon surface . These images confirm that the mean thickness of thin film was found to be (1.4-5.3 µm). Apart of this, the combination of cadmium and lead sulphide nanocomposites formed on porous silicon contributes to improve the performance of photodetector device [24].

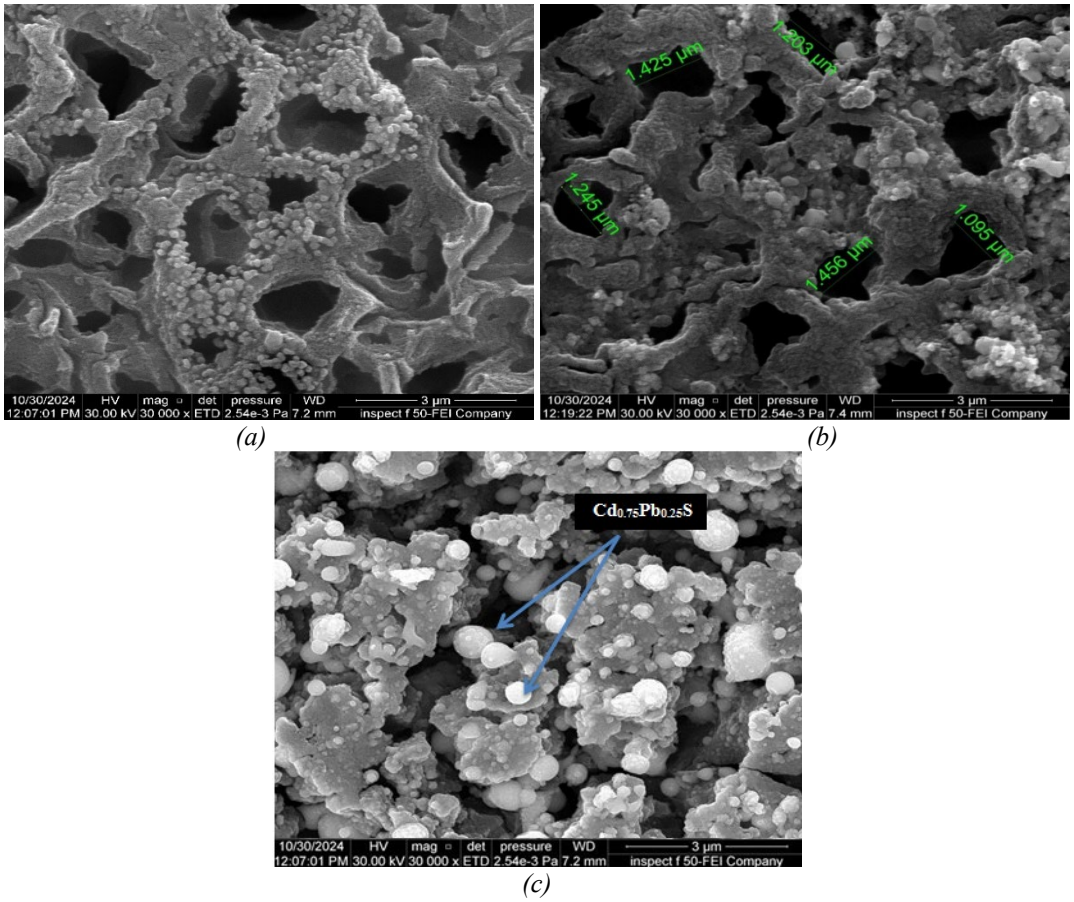

(a) *(b)*

(c)

Fig. 6. SEM of $Cd_xPb_{1-x}S$/porous silicon (a) PSi at etching 15min, (b) x=0.25 (c) x=0.7.5.

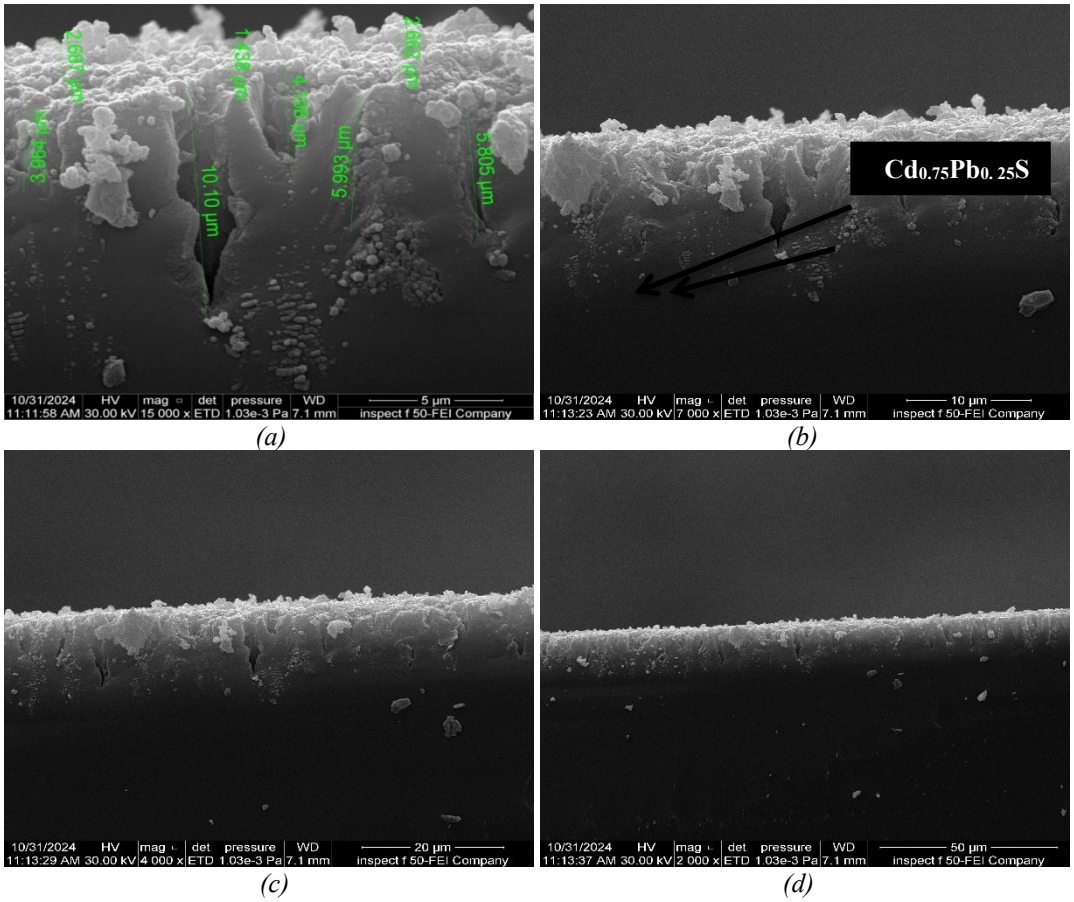

(a) *(b)*

(c) *(d)*

Fig. 7. Cross section of SEM of $Cd_xPb_{1-x}S$/porous silicon at x=0.75of various magnification (a) 15000x (b) 7000x (c) 4000x, (d)2000x.

3.3. Energy-dispersive X-ray (EDX)

The chemical structure of the porous silicon sample was scanned by EDX spectrum at etching time 5min as shown in Figure 8a. It is clear the strong signal was found to be Si and presence with a very small amounts from O and C elements [25]. Figure 8(b, c) exhibits EDX analysis of $CdxPb_{1-x}S$ thin films at composites x=0.25 and 0.5 respectively. It can be seen, the strong signals confirm presence Si, O and Pb elements and also weak signals were found to be Cd, S elements. On the other side, the dangling bonds of the elements mapping from C, Ca, Mg, Cl, Na were presented due to aggregation and formation solutions during preparation process [26]as Figure 8b. It is clear, the atomic percentage ratio of lead and cadmium sulphide gradually increased linearly at x=0.5. The strong peaks of elements were found to be Si, Pb, Cd & O. Conversely, the weak signals were found to be S, Cl, C, Al, Mg elements [27] as the as Figure 8c. also mapping color of EDX analysis of prepared elements can be observed as Figure 9 and Table 2,3&4.

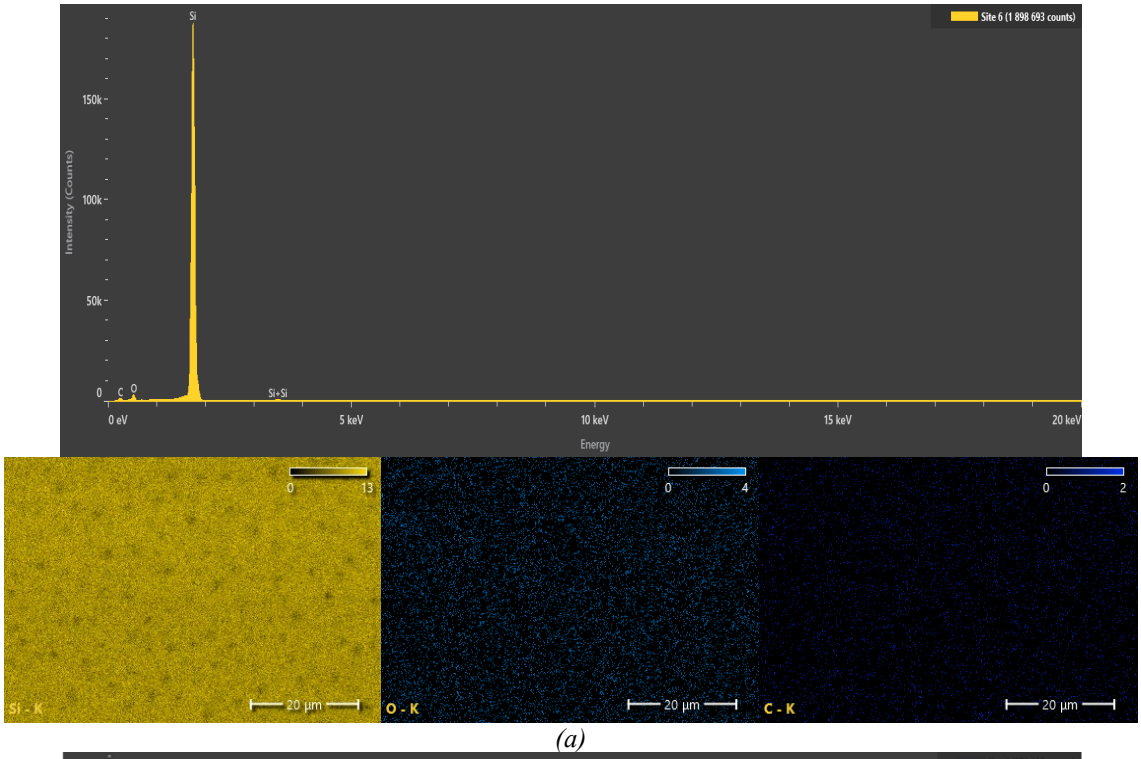

(a)

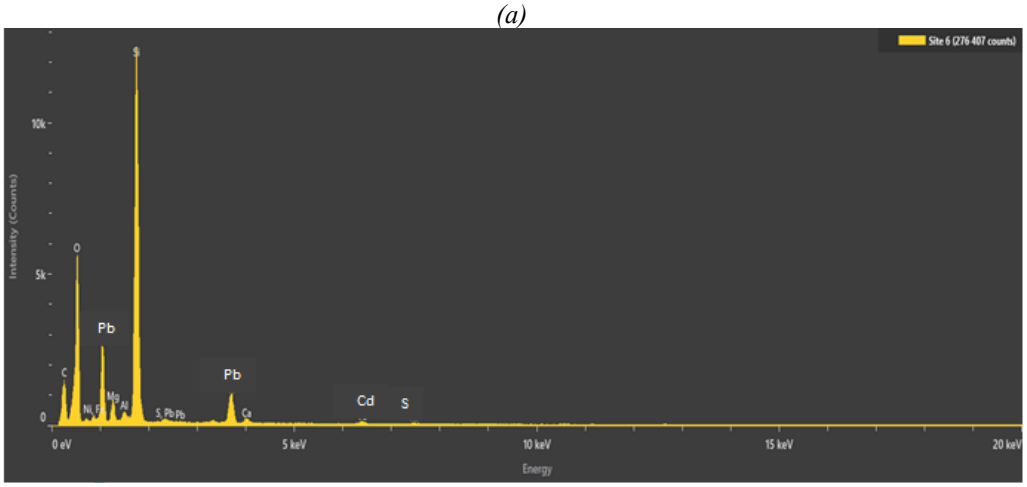

(b)

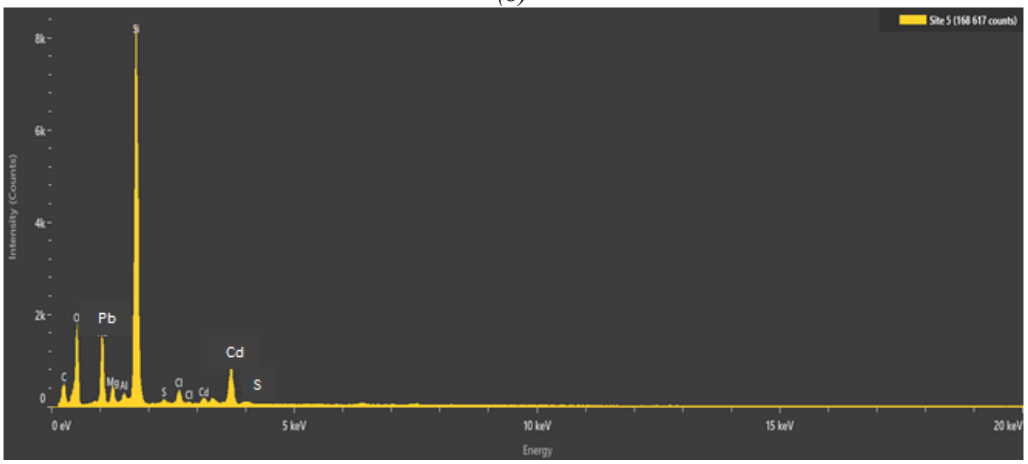

(c)

Fig. 8. EDX analysis of $Cd_xPb_{1-x}S$/porous silicon at etching time 5min of concentration (a) pure PSi, (b) x=0.25, (b) x=0.5.

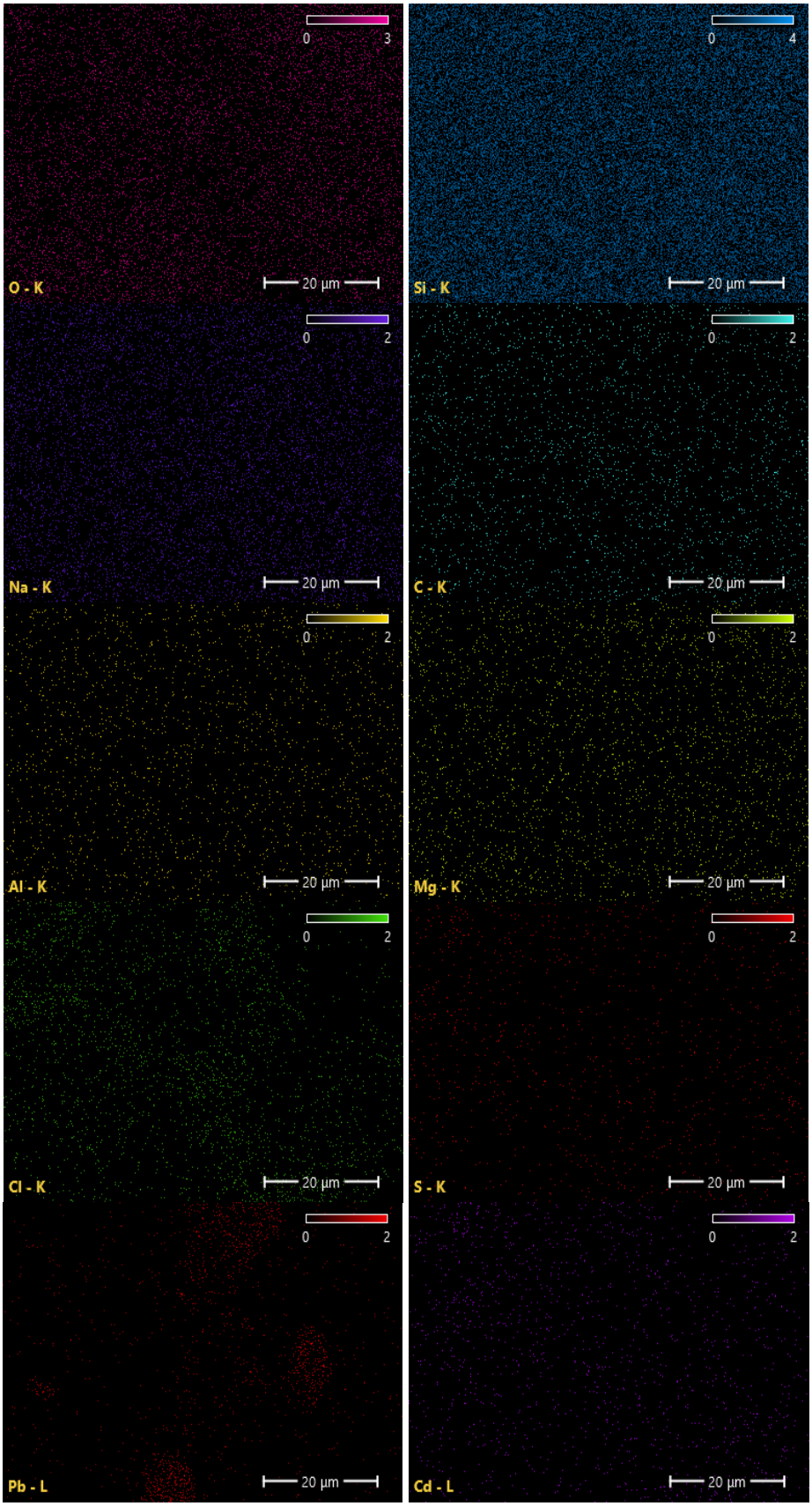

Fig. 9. Mapping color of EDX analysis of prepared elements.

Table 2. Data of elements of porous silicon at etching time 5min.

Element	Atomic Weight %
C	11.6
O	10.3
Si	78.1

Table 3. Data of elements of $Cd_xPb_{1-x}S$/porous silicon at concentration x=0.25.

Element	Atomic Weight %
Si	31.6
O	21.5
Cd	9.5
Pb	15.5
S	8.5
C	10.2
Na	2.2
Mg	0.5
ca	0.3
Al	0.2

Table 4. Data of elements of $Cd_xPb_{1-x}S$/porous silicon at concentration x=0.25.

Element	Atomic Weight %
Si	30.6
O	18.5
Cd	16.5
Pb	14.0
S	11.5
C	8.2
Mg	0.3
Al	0.2
CL	0.2

3.4. I-V characteristics

The electrical characteristics under dark and illumination conditions of the $Cd_xPb_{1-x}S$ thin films formed on porous silicon were observed at various composites (x=0,0.25,0.5,0.75,1) prepared using chemical spray method as Figures 10(a,b). It is clear that the acquired I-V curves have rectifying behavior due to presence of CdS and PbS thin film layer on porous silicon heterojunction n [28]. The current values of the prepared films increase with the increasing doped of Cd^{+2} ratio. Afterwards, increased reverse bias voltage was a significant increment in the current values due to absorbed photons caused an increment in current value at a higher bias voltage. which could be caused of raising in the depletion layer width. In accordance with this, the number of electrons in the CB of the doped films increased. It is also the important to note that the output of dark current increases of all samples with increasing Cd^{+2}concentration as a Figure 10b. Furthermore, the photocurrent current values also increased at illumination condition due to the photo-excited charge carriers at higher voltage [29]. Table 5 indicates the parameters of electrical properties. The results show the reverse saturation current density values increase with increasing concentration x as Figure 10c.

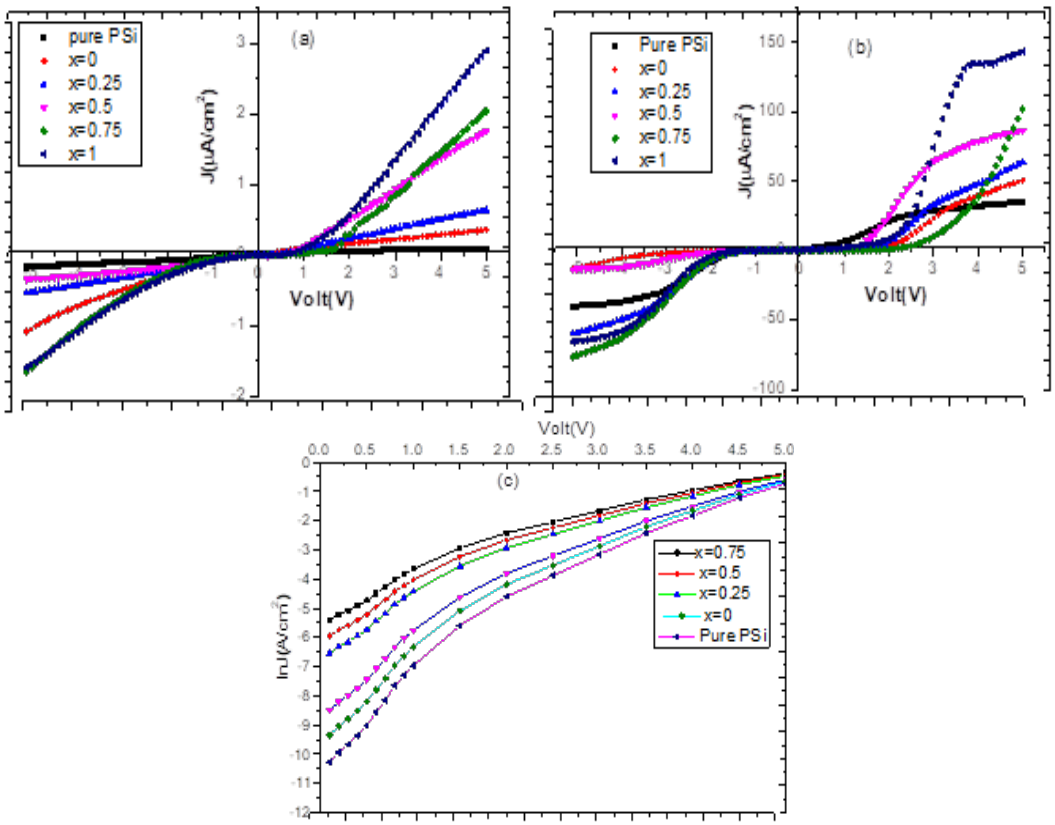

Fig. 10. I-V measurements of $Cd_xPb_{1-x}S$/porous silicon at various concentration (a) I-V under the dark, (b) I-V under the light, (c) relationship between ln J &Volt.

Table 5. Summarize parameter of I-V measurements of $Cd_{1-x}Pb_xS$/porous silicon thin films.

$Cd_{1-x}Pb_xS$/porous silicon			
Concentration x	**J_s (μA)**	**n**	**(eV)Φ**
Pure porous silicon	34.38	2.1	0.73
X=0	87.29	1.93	0.68
X= 0.25	204.65	1.81	0.62
X=0.5	1453.18	1.72	0.58
X=0.75	2632.02	1.61	0.53
X=1	4516.5	1.58	0.51

3.5. Photodetector

The photodetector performance of $Cd_{1-x}Pb_xS$/porous silicon thin films was measured at composites (x=0,0.25,0.5,0.75,1). The results show that the prepared films have good photosensitivity of all samples. The responsivity equation (R) can be calculated by the ratio of the output photocurrent to the input applied power as the following formula [30].

$$R = \frac{I_{ph}}{P \times A} \tag{5}$$

Additionally, the specific detectivity (D^*) can be evaluated as the following equation [31]:

$$D^* = \frac{R(\lambda)}{\sqrt{2qJ_{dark}}} \tag{6}$$

where J_d is the dark current density and q is the electron charge.

There are three peaks appearance in the responsivity and detectivity profile curves of the pure porous silicon substrate, the first peak at response in the range (350-400nm) at the ultraviolet region and the second region was observed at wide response (475−575 nm) at UV-visible. The third region at (750-850nm) located at the low response at IR region. The photodetector characteristics of the $Cd_xPb_{1-x}S$/porous silicon thin films were studied at (x=0,0.25.0.5,0.75,1). Two regions were observed at x=0, the first peak at high response and wide band at (475-575nm) and the second peak at low response (750-850nm). This is attributed that the lead sulphide (PbS) responses in range of (UV-vible). In contrast, the region at (350-400nm) was presented at x=1, this indicates to the cadmium sulphide (CdS) responses in the of ultraviolet region. Furthermore, the responsivity and detectivity values increase with increasing concentration x. The high values of Detectivity of $Cd_xPb_{1-x}S$/porous silicon thin films were found to be 1.19×10^{12}Jones, 1.31×10^{12} Jones, 2.18×10^{12} Jones, 3.92×10^{12}Jones, 1.53×10^{13}Jones, 1.06×10^{14} Jones at x=0,0.25,0.5, 0.75 and 1 respectively this is attributed to interface between the prepared thin film layer and porous silicon surface as Figure 11 and 12.

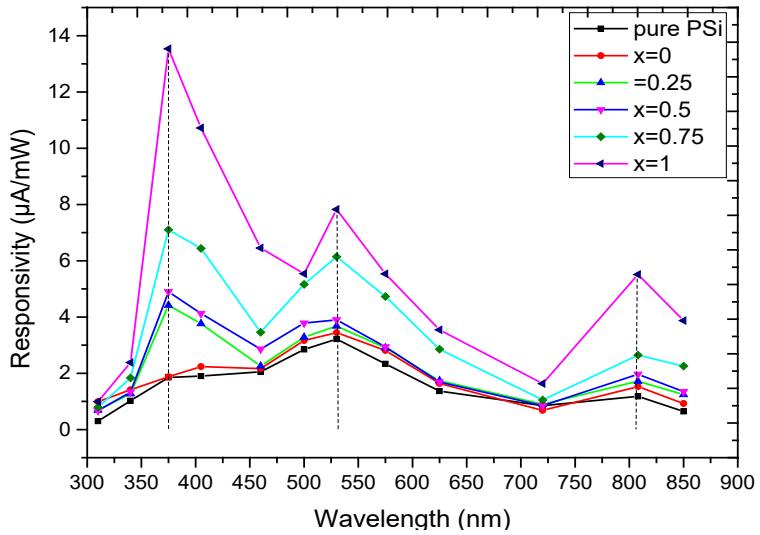

Fig. 11. Illustrates responsivity of $Cd_xPb_{1-x}S$/porous silicon thin films at various concentrations.

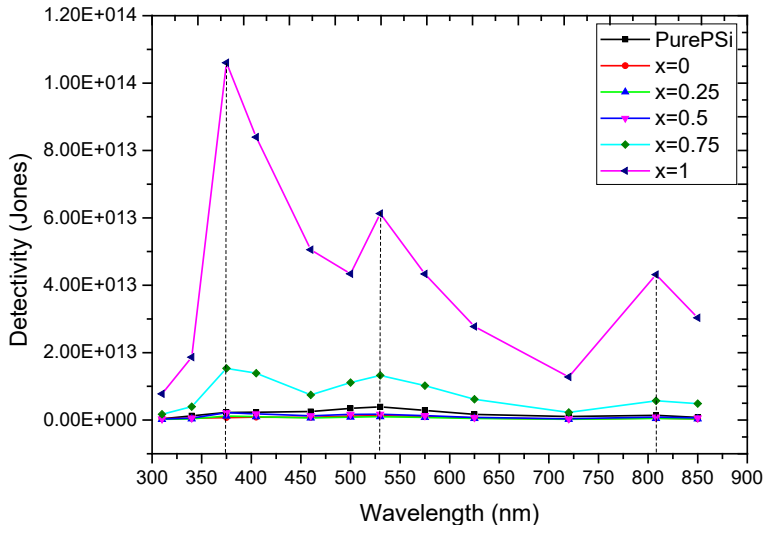

Fig. 12. Illustrates the detectivity of $Cd_xPb_{1-x}S$/porous silicon thin films at various concentrations.

The values of the quantum efficiency of $Cd_xPb_{1-x}S$/porous silicon thin films can be observed, It is clear that the efficiency increases with increasing concentration x. The high values of quantum efficiency were found to be 10%, 14%, 16%, 23% and 44% at x=0,0.25,0.5, 0.75and 1 respectively. This could be attributed to improve the reconfiguration of structure quality of the cadmium sulphide (CdS) deposited on porous silicon substrate at high concentration as Figure 13. Furthermore, the variation of photocurrent with time (time rise and time fall) was estimated to ensure the responsivity of the detector as Figure 14. Therefore, the results show that the deposited films have good photoconductivity and electrical stability under light cycling [32]. The values of time rise and time fall were found to be 0.32sec to 0.33sec respectively.

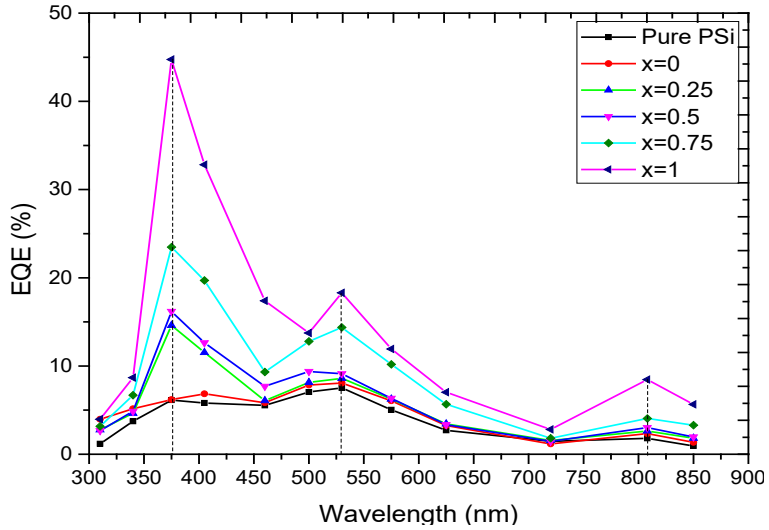

Fig. 13. Illustrates the efficiency of $Cd_xPb_{1-x}S$/porous silicon thin films at various concentrations.

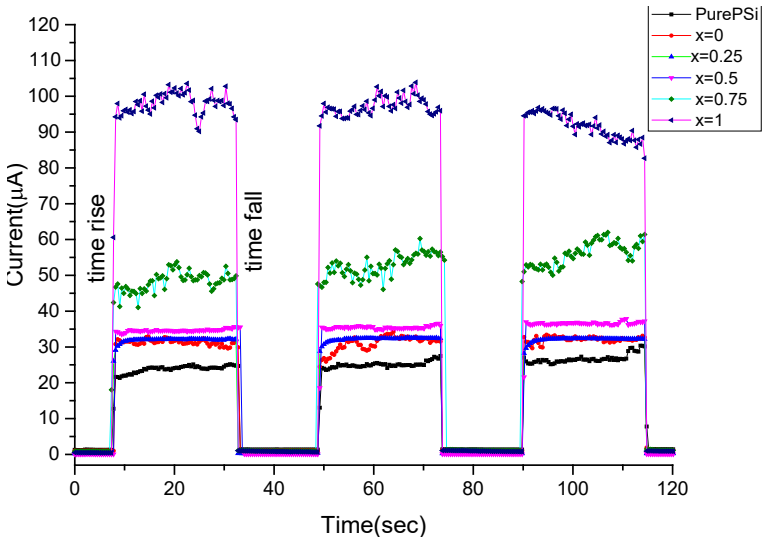

Fig. 14. Illustrates the time rise and time fall of $Cd_xPb_{1-x}S$/porous silicon thin films at various concentrations.

4. Conclusion

Nanocrystalline of CdS and PbS thin films can be successfully used in multi-junction photodetector devices. The structure properties indicate the presence of cubic and hexagonal phase structures of PbS and CdS thin films respectively. The morphological properties exhibit that the nanocomposites of lead and cadmium sulfide on porous silicon have spherical shape and uniform homogeneous of various concentration. Additionally, the particle diameter increases with increasing concentration. The dark and illumination current density of the prepared thin films have rectifying behavior and increase with increasing concentration. The photosensitivity characteristics of prepared $Cd_xPb_{1-x}S$/porous silicon thin films heterojunction showed the quantum efficiency increases with increasing concentration x. The high values of quantum efficiency were found to be 10%, 14%, 16%, 23% and 44% at x=0,0.25,0.5, 0.75and 1 respectively. In brief, $Cd_xPb_{1-x}S$/porous silicon thin films photodetector are effectively dependent on prepared requirements. Consequently, the experimental conditions can be used to manipulate the size and shape of the final structures.

References

[1] Omar Abdulazeez Alhamd, Ghazwan Ghazi Ali , Mutaz Salih Hasan Aljuboori,(2024), Trends in Sciences, 21(4), p.7402; https://doi.org/10.48048/tis.2024.7402

[2] Marwan Hafeedh Younus, Ghazwan Ghazi. Ali, Hesham Anwar Salih, (2021). Journal of Physics: Conference Series, 795,012002; https://doi.org/10.1088/1742-6596/1795/1/012002

[3] M. M. Abbas, A. A. Shehab, N. A. Hassan, (2011), Thin Solid Films, 519(15), pp: 4917-4922; https://doi.org/10.1016/j.tsf.2011.01.053

[4] J. Hernandez, Y. Vorobiev, R. Ramirez (2011), Solar Energy Materials & Solar Cells, vol.95, pp:1882-1888; https://doi.org/10.1016/j.solmat.2011.02.012

[5] V. Dhaval, Jaymin, K. Tapas, (2016). Advanced Science Letters, 22(4), pp:1022-1025; https://doi.org/10.1166/asl.2016.6948

[6] Hamid S. (2012), Applied Physics Research, 4(3); https://doi.org/10.5539/apr.v4n3p75

[7] H.P Wang, Z. Zhang, Y. Ning, X. Fang, IEEE Access, 7(2), (2018),19395-19400; https://doi.org/10.1109/ACCESS.2018.2885169

[8] Y. N. Al-Douri, C. Voon, Optik,147, (2017), 343-349; https://doi.org/10.1016/j.ijleo.2017.08.107

[9] G. G. Ali, M. A. Ahmed, A. A. Sulaiman, Digest Journal of Nanomaterials and Biostructures, 17(2), (2022), 473 – 480; https://doi.org/10.15251/DJNB.2022.172.473

[10] O. Bisia, O. Stefano, L. Pavesi, Science Reports 38(12), (2000), 1-126; https://doi.org/10.1016/S0167-5729(99)00012-6

[11] T. A. Aswad, T. A. Abbas, G. G. Ali, Digest J. of Nanomaterials and Biostructures 16 (3), (2021), 831-838; https://doi.org/10.15251/DJNB.2021.163.831

[12] J. Park, Y. Yanagida, T. Hatsuzawa, Sensors and Actuators B: Chemical, 233(11), (2016), 136-143; https://doi.org/10.1016/j.snb.2016.04.058

[13] U. M. Nayef, H. T. Hussein, A. M. Abdul Hussien, Optik 172(7), (2018),1134-1139; https://doi.org/10.1016/j.ijleo.2018.07.112

[14] J. Xu, Int. J. Electrochem. Sci., 14(2), (2019), 5188-5199; https://doi.org/10.20964/2019.06.10

[15] X. Yang, F. Xi Chen, X. S. Li, S. Li, X. Wan, W. Ma, Fuel Cells 21(1), (2020), 52-57; https://doi.org/10.1002/fuce.202000048

[16] H. Alaa, J. Abdul_Hussein, Sattar, (2020). Bas.J Sc., 40(1), pp: 162-177; https://doi.org/10.29072/basjs.20220110

[17] E. Nasir, M. Abass, (2016). Chalcogenide Letters, 13(2), pp: 271-279.

[18] B. Abdallah, A. Ismail, H. Kashoua, W. Zetoun, (2018), Journal of Nanomaterials, 10(1);

https://doi.org/10.1155/2018/1826959

[19] G. Lipika, G Jitupon, G. Rupkamal, C. Rupkamal, C. Minakshl (2022), Bull. Mater. Sci., 45(2), pp. 220.

[20] K. Omar, K.A. Salman, Journal of Nano Research,12(2) (2017), 123-134; https://doi.org/10.4028/www.scientific.net/JNanoR.46.45

[21] R. Vercauteren, Sensors and Actuators A: Physical, 318(12), (2020), 112486; https://doi.org/10.1016/j.sna.2020.112486

[22] O. S. Volovlikova, P. Lazarenko, Micromachines, 11(2), (2020), 199; https://doi.org/10.3390/mi11020199

[23] D. A. Lizunkova, I. A. Shishkin, N. V. Latukhina, IOP Publishing: Conference Series, 1 (2020), 1695; https://doi.org/10.1088/1742-6596/1695/1/012001

[24] Y. Tsai, Vacuum, 178(8), (2020), 109454; https://doi.org/10.1016/j.vacuum.2020.109454

[25] M. M. Hassan, M. A. Fakhri, Digest J. of Nanomaterials and Biostructures, 14 (4), (2019), 873-878.

[26] I. Sadovnikov, Russian Chemical Reviews, 88(6), (2019), 571-582; https://doi.org/10.1070/RCR4867

[27] Sh. T. Hezarjaribi, N. Shahruz, J. of Inorganic and Organometallic Polymers and Mater., 30, (2020),4072-4081; https://doi.org/10.1007/s10904-020-01556-z

[28] F. B. Mohammed Ameen, M. H. Younus, G. G. Ali (2024), Chalcogenide Letters, 21(4), pp:343-354; https://doi.org/10.15251/CL.2024.214.343

[29] A. A. Ahmed, G. G. Ali, N. A. Daham,(2024), Chalcogenide Letters, 21(1),pp:81-97; https://doi.org/10.15251/CL.2024.211.81

[30] Ghazwan Ghazi Ali, Ivan B. Karomi, Abdulkhaliq Ayuob Sulaiman, Abidalkarem M. Mohammed, (2020), Nuclear Inst. and Methods in Physics Research B 468 23-27; https://doi.org/10.1016/j.nimb.2020.02.022

[31] R. Ameni A. Chohdi, K. Ines (2024). J. Nanopart Res. (26), p. 47; https://doi.org/10.1007/s11051-024-05957-w

[32] S.H. Haneen, K.A. Nada (2021), Baghdad Science Journal,18(3):pp:640-648; https://doi.org/10.21123/bsj.2021.18.3.0640